Jour. Korean Inst. Mining Geol.
Vol. 26, No. 3, p. 279-287, 1993.

Mode of Occurrences and Depositional Conditions of Stannite from the Yeonhwa 1 Mine.

Je-Il Chung*

ABSTRACT: In the zinc-lead (-silver) ores from the Yeonhwa 1 mine, stannite is widespread, though minor in amount. It may be divided largely into two species on the basis of its chronological order during mineralization; i.e., stannite I formed in Stage I, and stannite II formed in Stage II. Also, the mineral may be classified into two types according to the difference of its associates; i.e., stannite 1 closely associated with sphalerite, and stannite 2 with galena. In general, the stannite 1 tends to predominate in the stannite I and the stannite 2 in the stannite II.

The formation temperature and sulphur fugacity of stannite 1 deduced from stannite-sphalerite geothermometry are from 280 to 350℃ and from 10^{-11} to 10^{-8} atm.

INTRODUCTION

The crystal structure of stannite (Cu_2FeSnS_4) may derive from the chalcopyrite structure, in which if half of the iron atoms in chalcopyrite are replaced by tin, stannite is built up. Zinc may also substitute for iron in stannite and the mineral kesterite (Cu_2ZnSnS_4) results. It has long been believed that a complete solid solution series may exist between stannite and kesterite, however, recent studies on natural minerals in the synthetic system Cu-Fe-Zn-Sn-S have revealed that complete solution series may exist at temperatures above 680℃. But below this temperature, there is miscible gap represented by the two-phase region (Springer, 1972; Harris and Owens, 1972; Petruk, 1973).

The marked difference in physical properties, especially in optical properties recognized between stannite and kesterite has already been noted by previous investigators.

With respect to the natural occurrence of stannite-kesterite intergorwths, on the other hand, Harris and Owens (1972) carried out the electron microprobe study and revealed that the guest phase has a composition $St_{59}Ke_{41}$(mole percent of stannite and keseterite molecules), whereas matrix (the host phase) has a composition $St_{35}Ke_{65}$, and that after annealing at 350℃, the samples appear to be homogenized. They considered that the above intergrowth texture was due to exsolution during cooling. Subsequentry, in the study on sulphides from the Mt. Pleasant mine, Petruk (1973) found the intergrowths of stannite($St_{45}Ke_{55}$) and kesterite(St24Ke76). Taking this result together with that given by Harris and Owen (1972) into account , he suggest that wider two-phase field is expected than proposed by Springer (1972). More recently, Hall et al.(1978) have examined the natural kesterite($St_{29}Ke_{73}$) and the coexisting stannite by single-crystal X-ray diffraction, and revealed that the two minerals are not isostructural; i.e., space group, stannite: $I\bar{4}2m$, kesterite: $I\bar{4}$. Unit-cells of these two phases are shown in Fig. 1.

Quite recently, Sugaki et al.(1983) have reexamined the phase relations in the pseudo-binary system stannite-kesterite and revealed that, at temperature 600℃, there exists intermediate solid solution(iss), which has intermediate composition between stannite and kesterite in addition to stannite s.s. and kesterite s.s., indicating that phase relation in this pseudo-binary system is not simple (Fig. 2).

An occurrence of stannite at Yeonhwa 1 has already been reported by Lee, S.R.(1980), however, unfortunately information on its physical properties and chemical compositions are scanty.

OCCURRENCE

In the zinc-lead (-silver) ores from the Yeonhwa 1 mine, stannite is widespread, though minor in amount. It may be divided largely into two species on the basis of its chronological order during mineralization; i.e., stannite I formed in Stage I, and stannite II formed in Stage II. Also, the mineral may be classified into two types according to the difference of its associates ; i e., stannite 1 closely associated

* Department of Geology, Chonbuk National University, Chonju 560-756, Korea

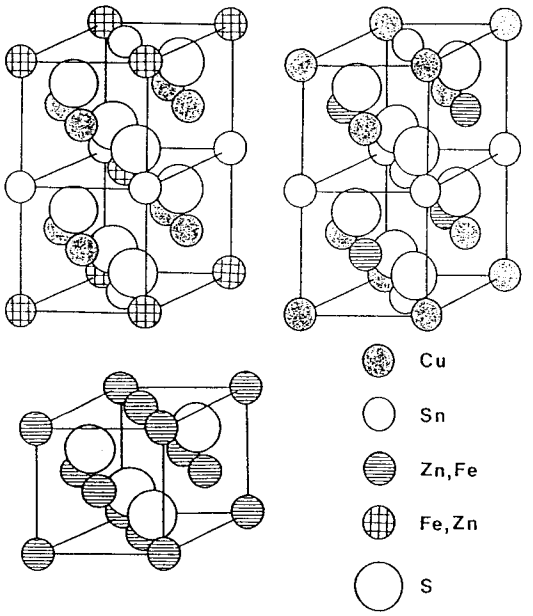

Fig. 1. Diagrammatic representation of stannite (upper left), kesterite (upper right) and sphalerite (lower left) structures, emphasizing the difference in metal ordering. The radius of the spheres is arbitrary (after Hall et al., 1978).

with sphalerite, and stannite 2 with galena. In reflected light, the stannite 1 exhibits greenish grey colour. In grneral, the stannite 1 tends to predominate in the stannite I and the stannite 2 in the stannite II. In rare cases, the stannite contains chalcopyrite blebs formed probably due to exsolution upon cooling, but sphalerite inclusion are not recognized at all.

Under the ore microscope, the stannite was observed in the followingtextural relationships.

(1) The discrete grains of stannite enclosed perfectly within the sphalerite host with coarse-grained as large as more than 1 mm across may be usually encountered. This mode of occurence is representative and most common at Yeonhwa 1. Individual crystals of it have quite irregular outline and attain 50 μm across (Fig. 3(1)).

(2) In some ore specimens in Stage I, irregularyshaped minute grains of stannite, usually with vermicular or skeletal shape, are sparsely distributed in the sphalerite host together with those of chalcopyrite and pyrrhotite. These minute inclusions of stannite, chalcopyrite and pyrrhotite may be attributed to exsolution products upon cooling (Fig. 3(2)).

(3) In coarse-grained pyrite- and galena-rich ores formed in Stage II containing abundant rhodochrosite as a gangue, there are sphalerite grains rimmed perfectly by stannite, showing apparently replacement texture. Such sphalerite grains also contain tiny dots of stannite, usually less than 10 μm across (Fig. 3(3)).

(4) In some zinc-lead ores rich in galena, the stannite grains with triangular form are intergrown intimately with galena having irregular shape. The stannite is relatively coarse-grained, attaining up to 70 μm across (Fig. 3(4)).

(5) In some pyrrhotite-rich ores with some galena and marcasite formed in Stage I, stannite often develops along the grain boundaries between pyrrhotite and galena. Individual grains stannite exibit narrow film or vermicular form, the width of which attain 20~30 μm (Fig. 3(5)).

(6) In rare cases, stannite II is in direct contact with boulangerite. These boulangerite-stannite intergrowths are usually scattered through the galena host. The boulangerite crystal is lath-shaped, attaining 10~20 μm in longer dimensions (Fig. 3(6)).

Optical and Physical Properties

As mentioned before, stannite I is greenish grey in colour, whereas stannite II is bluish grey. It has polishing hardness higher than galena and sphalerite. Between crossed polars, it is quite isotropic. No bireflectance and internal reflection were recognizable.

The reflectance measurements were performed using SiC standard. The wavelength dispersion of reflection for the wavelength of light between 420 and 700 nm by a 20 nm scans for the grain of stannite II-2 are listed in Table 2, together with the data for stannite given by Picot and Johan (1982). There is no significant departure between the two; reflectance increases gradually with increasing wavelength below 600 nm, but it decrease gradually with increasing wavelength above 600 nm.

The microhardnesses for some selected grains of the mineral were determined using Akashi MVK-F microhardness tester. The results thus obtained were expressed in terms of Vicker's hardness number (VHN), which ranged from 220 to 246 kg/mm^2 at a 50 g-load.

Chemical Composition

Chemical analysis of the present stannite was performed using an electron microprobe with wavelength dispersion mode (WDX). In this study, a JEOL "Superprobe JXA-733" was used. The ZAF corrections for matrix effects were made to the Castaing's

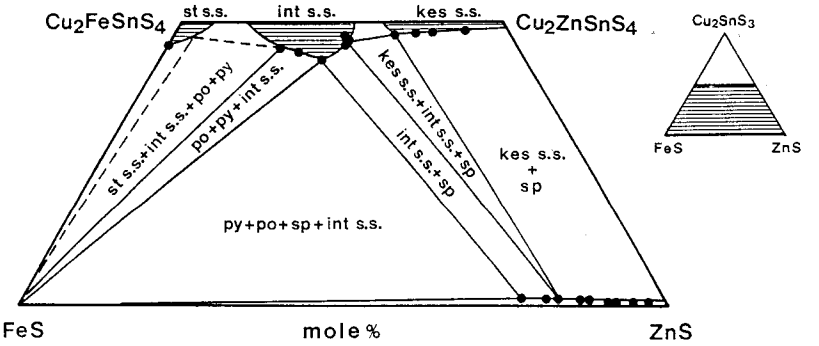

Fig. 2. Phase diagram in the system Cu_2SnS_3-FeS-ZnS at 600℃, log $f(S_2) = -2.3$ (after Sugaki et al.,1983). Abbreviations: kes; kesterite, po; pyrrhotite, py; pyrite, sp; sphalerite, and st; stannite.

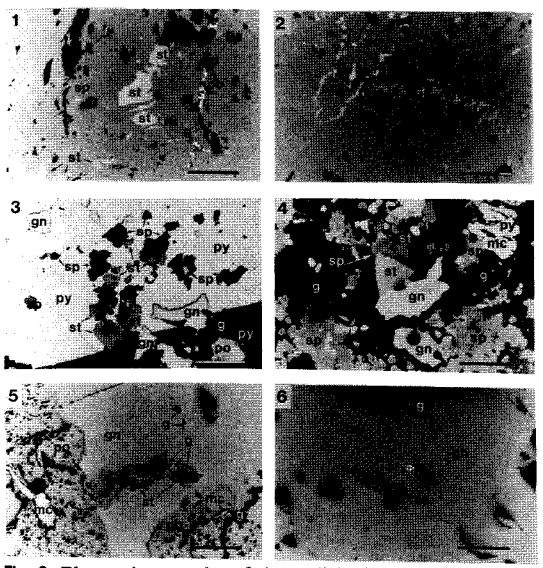

Fig. 3. Photomicrographs of the polished sections (one polar), showing the mode of occurrence of stannite. Bar scale indicates 100 m in length. Abbreviations: bl; boulangerite, cp; chalcopyrite, gn ; galena, mc; marcasite, po; pyrrhotite, py; pyrite, sp; sphalerite, st; stannite, and g; gangue mineral. 1; Specimen No. YH83-006, 2; Specimen No.YH83-002, 3; Specimen No. 54-004, 4; Specimen No. 12-111, 5; Specimen No. 24-108, and 6; Specimen No.YH 84-301.

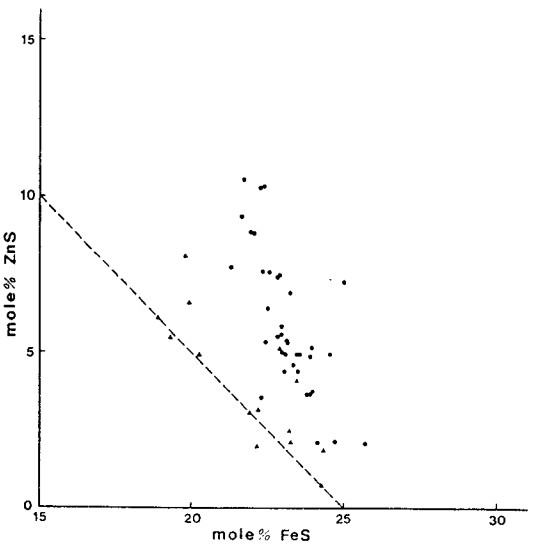

Fig. 4. Variation diagram showing the relation of ZnS versus FeS in stannite (mole percent). Full circle; stannite associated with sphalerite and full triangle; stannite not associated with sphalerite. Broken line means the value of (ZnS+FeS) mole percent=25 mole percent.

values at first approximation.

The qualitative microprobe analysis spectrometer scans detected the elements of Cu, Fe, Zn, Sn and S. Concentrations of other elements which were expected to enter into the stannite structure, such as In and Cd were less than the detection limits of microprobe, althogh careful peak search of charactristic X-rays from these elements was made.

The quantitive analyses of the stannite by microprobe were made for fifty three spot in discrete nineteen grains from eight ore specimens, from which it is evident that the Yeonhwa 1 stannite is "Zn-bearing stannite". Also , in Fig. 4, the analytical results are plotted in terms of FeS versus ZnS into the FeS-ZnS diagram, in which stoichiometric composition $Cu_2(Fe, Zn)SnS_4$ represents a straight line connectioning 25 mole percent FeS and 10 mole percent ZnS. From this figure, it is clearly seen that the stannite 1 has the concentration of ZnS in excess for the stoichiometric composition; i.e.,(FeS+ZnS)>25 mole pe-

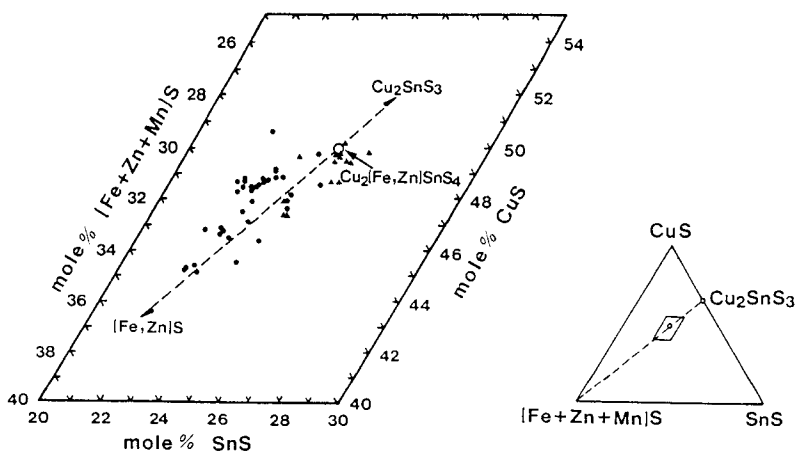

Fig. 5. The enlarged parallelogram in the triangle of the pseudo-ternary system CuS-(Fe+Zn+Mn)S-SnS, showing the composition of stannite. Open circle; stoichiometric stannite (Cu_2(Fe, Zn)SnS_4), full circle; stannite associated with sphalerite, and full triangle; stannite not associated with sphalerite. Broken line connects the composition of stoichiometric Cu_2(Fe, Zn)SnS_4 and extends toward the compostion of stoichiometric Cu_2SnS_3 and (Fe, Zn)S.

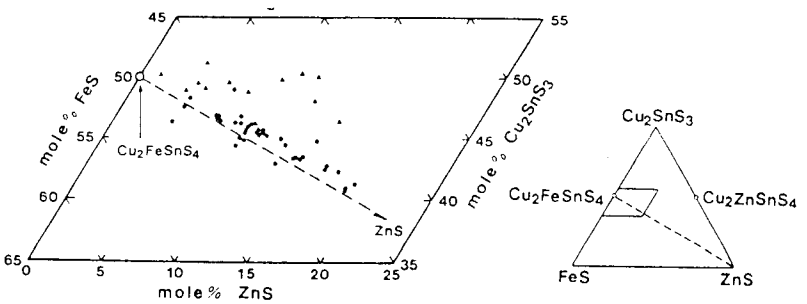

Fig. 6. The enlarged parallelogram in the triangle of the pseudo-ternary system Cu_2SnS_3-FeS-ZnS showing the composition of stannite. Open circle; stoichiometric stannite (Cu_2(Fe, Zn)SnS_4), full circle; stannite associated with sphalerite, and full triangle; stannite not associated with sphalerite. Broken line connects the composition of stoichiometric Cu_2(Fe, Zn)SnS_4 and extends toward the composition of stoichiometric Cu_2SnS_3 and (Fe, Zn)S.

rcent. In marked contrast, stannite 2 is plotted adhering to the straight line, indicating that (FeS+ZnS)≃ 25 mole persent, in other words (FeS+ZnS)≃ 1 in the formula of the stoichiometirc stannite 2CuS·(Fe, Zn)S·SnS.

In order to clarify the above-mentioned compositional features of the stannite in relation to crystal structure, the chemical data were processed in the following procedures. The chemical compositionals of the stannite were plotted into the triangle diagram of the system CuS-(Fe+Zn+Mn)S-SnS in Fig. 5. In this system, Cu, (Fe+Zn+Mn) and Sn must lie at a point stoichiometric composition Cu_2(Fe, Zn, Mn) Σhnh/. It is found from this figure that points of stannite 1 deviate significantly from this point, those of the stannite 2 do not deviate, except a few instances.

Taking the compositional features of the stannite as mentioned before, their chemical compositions were plotted into the triangle diagram CuS_2SnS_3-FeS-ZnS, as shomn in Fig. 6, from which it is seen that plots of the stannite 1 lie near the line connecting stannite (Cu_2FeSnS_4) with sphalerite (ZnS), whereas plots of the stannite 2 lie near the line connecting stannite with kesterite.

Thus, it becomes clear that the Yeonhwa 1 stannite are "Zn-bearing stannite" and may be divided into two types, the stannite 1 and stannite 2 ; the former belongs to stannite-sphalerite series, whereas the latter to stannite-keserite series. Probably, stannites are partially ordered compound with respect to metals, (Fe+Zn), Cu and Sn. Further investigation by X-ray diffraction is needed.

Summary with Some Comments

Table 1. Information on the specimens containing stannite analyzed with electro microprobe.

Specimen No.	Name of deposit	Occurrence site	Mineral assemblage	Type
YH83-006	Dongjeom	−60 m level	sp-po-gn-cp-st	A
YH83-002	Dongjeom	−60 m level	sp-gn-st-cp	A
24-114	Myobong	−240 m level	sp-po-mc-st	A
54-209	Namsan	−540 m level	py-po-cp-gn-ap-st-mc	A
YH83-109	Dongjeom	−120 m level	sp-py-cp-st	A
54-004	Namsan	−540 m level	py-sp-st-gn-po-mc	B
12-111	Wolam	−120 m level	po-py-gn-sp-cp-mc-st	B
YH83-105	Dongjeom	−120 m level	ap-sp-cp-gn-st	B

A; contacted with sphalerite and B; no contacted with sphalerite.

Table 2. Reflectance in air for stannite.

Wavelength λ_o(nm)	Reflectance (R percent) (1) $R_{max.}$	(1) $R_{min.}$	(2) $R_{max.}$	(2) $R_{min.}$
420	23.1	21.6	22.0	20.0
440	24.4	22.2	23.6	21.5
460	25.7	23.5	24.9	23.0
480	26.8	24.7	26.0	24.3
500	27.5	25.4	27.1	25.5
520	27.9	26.1	28.0	26.5
540	28.2	26.7	28.6	27.4
560	28.5	27.3	29.0	28.0
580	28.8	27.3	29.4	28.6
600	29.1	27.7	29.5	28.8
620	28.7	27.6	29.5	29.0
640	28.2	26.9	29.2	28.8
660	27.6	26.0	28.6	28.2
680	27.4	25.9	27.8	27.6
700	27.5	25.8	26.8	26.4

1; Yeonhwa 1 mine, Specimen No. 54-004. Stendard; SiC. Spot size of light beam; 20 $\mu m\phi$ and objective; X20. Numerical aperture; 0.40. 2; After Picot and Johan (1982).

The marked discrepancy in the shapes of miscible gap (two phase region) recognized in the phase diagram along the stannite-kesterite series obtained by synthetic work by Springer (1972) and by the works on natural intergrowths of these two phases by Harris and Owens (1972) and Petruk(1973) has not been fully explained hitherto. In this respect, Kato (1974) suggests the following two possibilities. The first is that the synthetic α-form of Cu_2FeSnS_4, into which the β-form is transformed 680℃ has sulphur deficiency (Franz, 1971). The second is that the α-form obtained by experiment is not perfectly ordered, but is partially ordered, which has sphalerite substructure. In addition to the above mentioned matters, the phase diagram of the synthetic stannite-kesterite series given by Sugaki et al. (1983) suggests the more complicated features for the phase relation along this pseudo-binary join in the system Cu-(Fe, Zn)Sn-S than considered before.

As indicated in Fig. 2, at temperature 600℃, stannite s.s. cannot coexist with sphalerite s.s. in equilibrium. As mentioned before, however, direct contact of Zn-bearing stannite with sphalerite is most common in natural occurrence. Iron and zinc partitioning between coexisting Zn-bearing stannite and sphalerite s.s. as a possible indicator of temperature and sulphur fugacity has been discussed by Nekrasov et al. (1979) and Nakamura and Shima (1982), and the application of this "stannite-sphalerite geothermometer" to the natural occurrence was attempted by Shimizu and Shikazono (1985). The application of this to the Yeonhwa 1 zinc-lead (-silver) ores will be mentioned below this paper.

STANNITE-SPHALERITE GEOTHERMOMETRY

General Statements

Iron and zinc partioning between stannite and sphalerite may be expressed by the following exchange reaction.

$$Cu_2FeSnS_4 \text{ (in stannite)} + ZnS \text{(in sphalerite)} \Leftrightarrow Cu_2ZnSnS_4 \text{ (in stannite)} + FeS \text{ (in sphalerite)} \quad (1)$$

The partition coefficient, *Kd*, for reaction in the above Eq.(1) is given by,

$$Kd = [(X^{st}Cu_2FeSnS_4)/(X^{st}Cu_2ZnSnS_4)]/(X^{sp}FeS/X^{sp}ZnS) \quad (2)$$

where X^a_i denotes mole fraction of component *i* and *a* the phases concened (stannite (*st*) and sphalerite (*sp*) in this case).

Nekrasov et al. (1979) and Nakamura and Shima (1982) reported the following relations showing a temperature dependency of iron and zinc partitioning

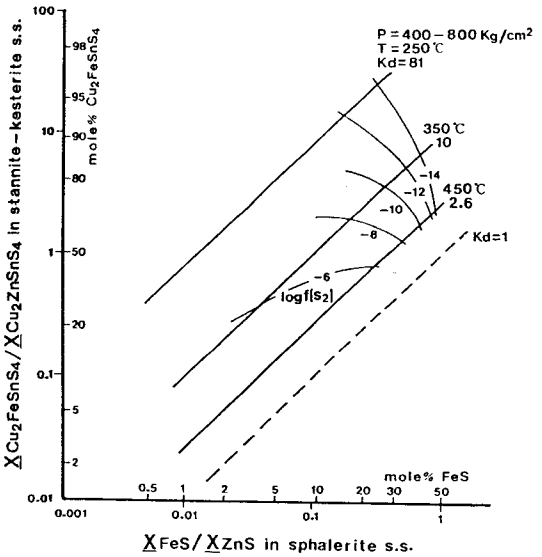

Fig. 7. Diagram showing the relation between $X_{Cu_2FeSnS_4}/X_{Cu_2ZnSnS_4}$ in zincian stannite and X_{FeS}/X_{ZnS} in Fe-bearing sphalerite (after Nakamura and Shima, 1982).

in stannite-sphalerite pair,

$$\log Kd=(1.274\times10^3\times T^{-1})-1.174, \quad \text{(Nekrasov. et al., 1979)} \tag{3}$$

$$\log Kd=(2.8\times10^3\times T^{-1})-3.5. \quad \text{(Nakamura and Shima, 1982)} \tag{4}$$

The above two geothermometers are in good agreement at about 380℃, but at lower and higher temperature regions, the difference in log *Kd-T* relation determined from Eqs. (3) and (4) becomes conspicuous.

Shimizu and Shikazono (1985) have recognized that, there is good correlation between stannite-sphalerite temperatures based on Eq. (4) and homogenizing temperatures of fluid inclusions and sulphur isotope temperature, and stressed that the stannite-sphalerite pair is useful indicator of temperature and sulphur fugacity, $f(s_2)$. Moreover, they have shown the results on three types of ore deposits (mostly Japanese ones) and deduced that the formation temperatures are not significantly different for skarn-type, polymetallic vein-type and Sn-W vein-type deposits,

Table 3. Selected electron-microprobe analyses of stannite associated with sphalerite.

Po.	Gr.	Weight percent							$\log \frac{X_{Cu_2FeSnS_4}}{X_{Cu_2ZnSnS_4}}$
		Cu	Fe	Zn	Mn	Sn	S	Total	
1	A	27.40	12.57	4.25	–	26.88	28.95	100.05	0.58
2	A	29.33	12.41	2.64	–	26.99	29.28	100.65	0.52
3	B	27.81	11.63	5.89	0.60	25.90	29.67	101.50	0.36
4	B	27.50	11.63	6.55	0.03	25.75	29.37	100.83	0.32
5	C	30.07	11.84	2.17	0.02	27.61	29.19	100.90	0.79
6	C	27.38	11.82	6.39	0.01	25.24	29.21	100.05	0.33
7	C	27.81	11.39	5.42	0.08	24.57	29.51	98.78	0.39
8	E	28.79	12.33	4.73	0.14	25.80	29.77	101.56	0.56
9	E	29.10	12.34	2.70	0.13	25.93	29.48	99.68	0.73
10	E	28.35	12.16	4.64	0.17	26.18	29.80	101.30	0.48
11	E	29.54	12.22	3.52	0.15	26.06	29.74	101.23	0.61
12	F	29.59	12.43	2.84	0.14	26.09	29.65	100.74	0.70
13	F	29.17	12.25	3.42	0.14	25.81	29.94	100.73	0.63
14	F	29.59	11.99	3.98	0.17	25.13	30.29	101.12	0.54
15	H	27.38	11.82	6.39	0.01	25.24	29.21	100.05	0.34
16	H	27.81	11.39	5.42	0.08	24.57	29.51	98.78	0.39
17	H	29.25	12.39	2.27	0.01	25.82	29.47	99.20	0.81
18	I	29.14	12.38	2.28	0.01	26.38	29.72	99.91	0.81
19	I	28.83	11.89	3.52	0.02	25.47	29.46	99.19	0.61
20	J	29.26	12.78	2.34	0.03	27.66	29.61	101.65	0.79
21	K	29.25	12.25	2.72	0.13	26.12	29.71	100.18	0.72
22	K	29.32	12.16	3.45	0.14	26.00	30.18	101.25	0.23
23	K	29.32	12.59	3.16	0.17	25.34	30.25	100.83	0.68
24	L	28.12	11.87	4.77	0.22	25.63	29.98	100.59	0.46
25	L	29.41	12.16	2.74	0.13	26.31	29.95	100.70	0.72

Po.; point number, Gr.; grain number, point no. 1~7; specimen no. YH83-006, point No. 9~14L; specimen no. YH83-002, point no. 15~19; specimen no. 54~209. point no. 20; specimen no. 24~114, and point no. 21~25; specimen no. YH83-019.

Table 4. Selected electron-microprobe analyses of sphalerite associated with stannite.

Po.	Gr.	Weight percent							$\log \frac{X_{FeS}}{X_{ZnS}}$
		Zn	Fe	Mn	Cu	Cd	S	Total	
1	A	56.12	9.70	0.12	0.05	0.35	33.36	99.70	−0.69
2	A	56.99	9.43	0.09	0.06	0.34	33.49	100.40	−0.72
3	B	56.23	9.46	0.06	0.35	0.39	33.23	99.72	−0.71
4	B	55.87	9.86	0.09	0.69	0.06	33.41	99.98	−0.68
5	C	56.58	10.14	0.10	0.64	0.38	33.34	101.18	−0.66
6	C	56.73	10.10	0.10	0.16	0.33	33.32	100.74	−0.69
7	C	56.88	9,82	0.12	0.10	0.34	32.76	100.02	−0.70
8	E	53.59	10.56	2.07	0.22	0.38	33.77	100.59	−0.64
9	E	53.18	10.94	1.90	0.16	0.39	34.05	100.62	−0.63
10	E	52.16	11.25	2.63	0.05	0.39	34.00	100.48	−0.60
11	E	51.88	11.57	2.04	0.19	0.36	34.12	100.16	−0.57
12	F	52.89	10.80	.1,40	0.28	\0.39	34.35	100.11	−0.63
13	F	52.44	11.14	1.90	0.16	0.34	34.02	100.00	−0.60
14	F	53.10	11.28	1.98	0.05	0.35	33.59	100.35	−0.61
15	H	57.18	9.72	0.10	0.09	0.41	33.24	100.74	−0.69
16	H	57.18	9.78	0.09	0.06	0.36	33.07	100.54	−0.70
17	H	56.20	10.02	0.18	0.04	0.30	32.91	99.65	−0.69
18	I	56.64	9.99	0.15	0.06	0.35	33.01	100.20	−0.69
19	I	57.48	9.37	0.10	0.09	0.37	33.18	100.95	−0.79
20	J	56.14	9.80	0.12	0.05	0.35	33.24	99.70	−0.69
21	K	56.84	9.44	0.07	0.68	0.40	33.32	100.75	−0.72
22	K	55.94	10.10	0.12	0.14	0.31	33.19	99.80	−0.69
23	K	56.14	9.80	0.12	0.05	0.35	33.24	99.70	−0.69
24	L	56.25	9.55	0.06	0.35	0.39	33.11	99.71	−0.69
25	L	55.88	9.96	0.09	0.69	0.06	33.29	99.97	−0.68

Po.; point number, Gr.; grain number, point no. 1~7; specimen no. YH83-006, point no. 9~14L; specimen no. YH83-002, point no. 15~19; specimen no. 54~209, point no. 20; specimen no. 24~114, and point no. 21~25; specimen no. YH83-019.

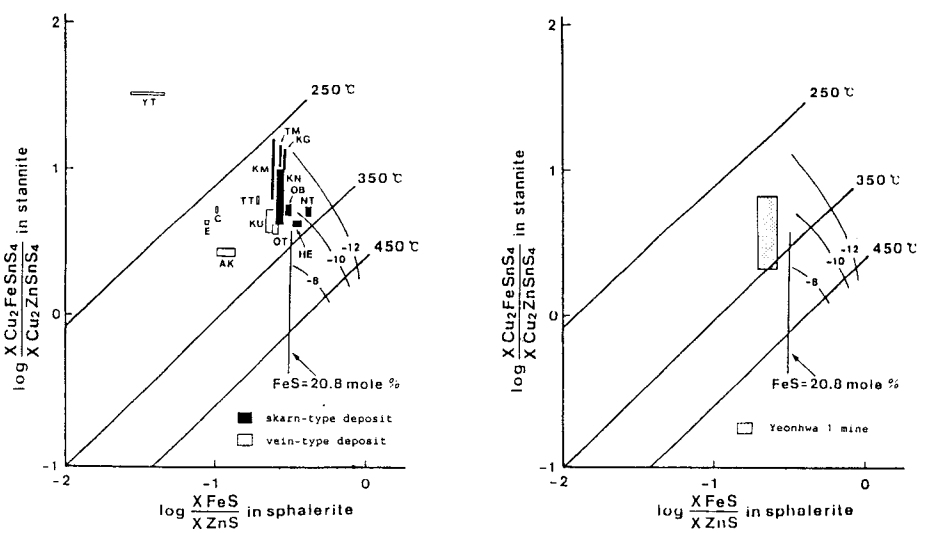

Fig. 8. Log(X_{FeS}/X_{ZnS}) sphalerite-log($X_{Cu_2FeSnS_4}/X_{Cu_2ZnSnS_4}$) stannite diagrams showing the distribution of each deposit of them. Skarn and vein type (left, after Shimizu and Shikazono, 1985) and Yeonhwa 1 mine (right). Abbreviations: KM; Kamioka, OB; Obira, KN; Kano, KG; Kuga, TM; Tsumo, OT; Ohtani, KU; Kaneuchi, AK; Akenobe, TT; Takatori, HE; Hoei, YT; Yatani, NT; Nakatatsu, C; Cornwall, and E; East.

whereas the sulphur fugacities are different.

As mentioned above, in the Yeonhwa 1 zinc-lead (-silver) ores, the coexistence of Zn-bearing stannite with Fe-bearing sphalerite is common, and occasionally direct contact of the two minerals may be obseved. If the assumption is made here that the mineral pair is in equlibrium, their compositions near the contact will serve as indicator of the formation temperature and sulphur fugacity (Fig. 7).

Analytical Procedures

The mutal contacts between Zn-bearing stannite and Fe-bearing sphalerite were searched under the ore microscope on polished sections, taking both optical and compositional homogeneity into consideration, and the area containing the exotic particles, such as chalcopyrite in Fe-bearing sphalerite was avoided. Moreover, analytical points of the mineral pair were selected as near as possible.

Then careful microprobe analyses for the mineral pair were carried out. The pairs, in which Fe-bearing sphalerite containing manganese more than 1 weight percent Mn were avoided.

Results and Discussion

The results of microprobe analyses for the Zn-bearing stannite and Fe-bearing sphalerite are listed in Table 3 and Table 4. In addition, they are shown diagramatically in Fig. 8 (right), showing the relations between $\log(^{x}Cu_2FeSnS_4/^{x}Cu_2ZnFeSnS_4)st$ and $\log(^{x}FeS/^{x}ZnS)sp$ for the Yeonhwa 1 materials, together with the diagram given by Shimizu and Shikazono (1985) on some ore deposits of skarn type, polymetallic vein type and of Sn-W vein type.

As shown in Fig. 8 (right), the elongated rectangle showing the range of the plots, temperature ranges from about 280 to 350℃ and sulphur fugacity from about 10^{-11} to 10^{-8} atm, which correspond to those of the Japanese skarn type ore deposits.

ACKNOWLEDGEMENT

Author would like to thank professor N. Imai of Waseda University for his useful guidances, discussions and advices.

This research was partly supported by the Center for Mineral Resource Research sponsored by the Korea Science and Engineering Foundation.

REFERENCES

Hall, S. R., Szyam, S. T. and Stewart, J. M. (1978) Kesterite, $Cu_2(Zn, Fe)SnS_4$, and stannite $Cu_2(Fe, Zn)SnS_4$, structurally similar but distinct minerals. Canad. Minerl., v. 16, p. 131-139.

Harris, D. C. and Owens, D. R. (1972) A stannite-kesterite exolution from British Columbia. Canad. Minerl., v. 11, p. 531-534.

Imai, N. and Lee, H. K. (1980) Complex sulphide-sulposalt ores from Janggun mine, Republic of Korea. In "Complex sulphide ores" (Proc. Inter. Conf. for Complex Sulphide Ores), Rome, p. 248-259.

Kato, A. (1974) Sulphide minerals in the Cu-(Fe, Zn)-(Sn, In) system. Minerl. J., v. 11 (Special issure 2), p. 145-153.

Lee, S. R.(1980) Mineralogy of the lead-zinc deposits from the Yeonhwa 1 mine, Korea (in Korean). Unpub. Master Thesis to Graduate Sch. Seoul Nat. Univ..

Nakamura, Y. and Shima, H. (1982) Fe and Zn partitioning between sphalerite and stannite (abst. in Japanese). Coll. Abst. Autumn Joint. Meet., Miner. Soc. Japan, Soc. Mining Geol. Japan and Japanese Assoc. Miner. Petrol. Econ. Geol., A-8, p. 8.

Nekrasov, I. J., Sorokin, V. I. and Osadchii, E. G.(1979) Fe and Zn partitioning between stannite and sphalerite and its application in geothermometry. In: Origin and Distribution of the Elements. L. H. Ahrens, Ed., Phys. Chem. Earth, v. 34, p. 739-742.

Petruk, W. (1973) Tin sulphides from the deposit of Bruswick Tin Mine Limited. Canad. Minerl., v. 20, p. 46-54.

Picot, P. and Johan, Z. (1982) Atlas of ore minerals. Elsevier Press, 1st ed.

Shimizu, M. and Shikazono, N. (1985) Iron and zinc partitioning between coexisting stannite and sphalerite: a possible indicator of temperature and sulfur fugacity. Minerl. Deposita, v. 20, p. 314-320.

Springer, G. (1972) The pseudobinary system Cu_2FeSnS_4-Cu_2ZnSnS_4 and its mineralogical significance. Canad. Minerl., v. 11, p. 535-541.

Sugaki, A., Kitakaze, A. and Ootsuki, T. (1983) Equilibrium of Cu-Fe-Sn-S system (V) (abst. in Japanese). Coll. Abst. Autumn Joint Meet., Minerl. Soc. Japan, Soc. Mining Geol. Japan and Japanese Assoc. Minerl. Petrol. Econ. Geol., C-42, p. 140.

Manuscript received 31 May 1993

제 1 연화광산에서 산출되는 황석석의 산출상태와 생성환경

정 재 일

요 약: 제 1 연화 광산에서 산출되는 황석석은 생성 시기를 기준으로 하면 비교적 이른 시기 (Stage I)에 산출된 황석석 I (Stannite I)과 늦은 시기 (Stage II)의 황석석 II (Stannite II)로 나눌 수 있으며 산출상태를 기준으로 하여 섬아연석과 밀접히 공생하는 황석석 1 (Stannite 1)과 방연석과 밀접히 공생하는 황석석 2 (Stannite 2)로 나누어진다.

일반적으로 황석석 1은 황석석 I이 황석석 2는 황석석 II가 우세한 경향이 있다.

황석석-섬아연석 지질온도계를 이용하면 생성 온도는 280~350℃ 이며 유황의 분압은 10^{-11}~10^{-8} atm.으로 추정된다.

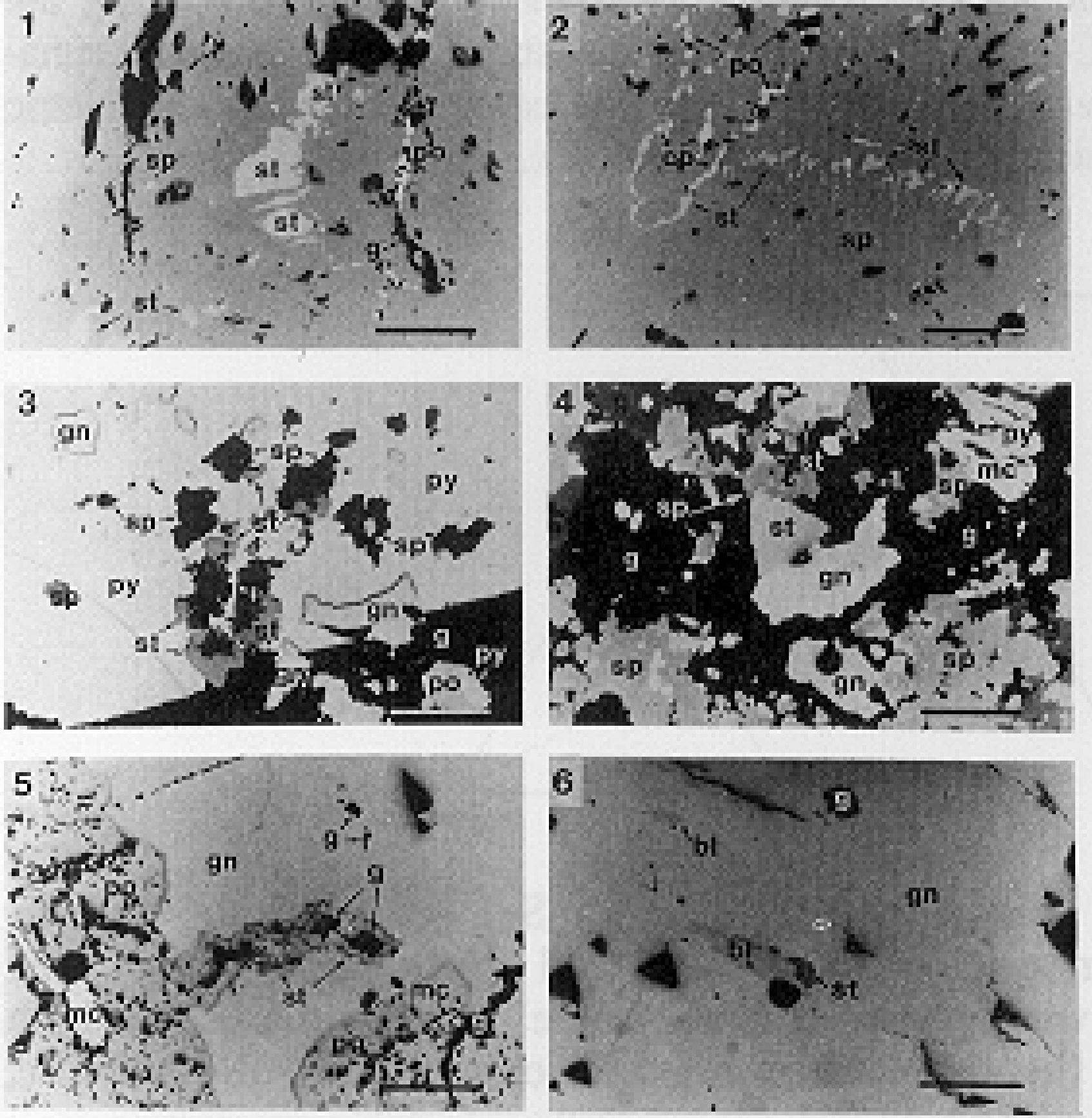

Fig. 3. Photomicrographs of the polished sections (one po-